

## Electronic supplementary information

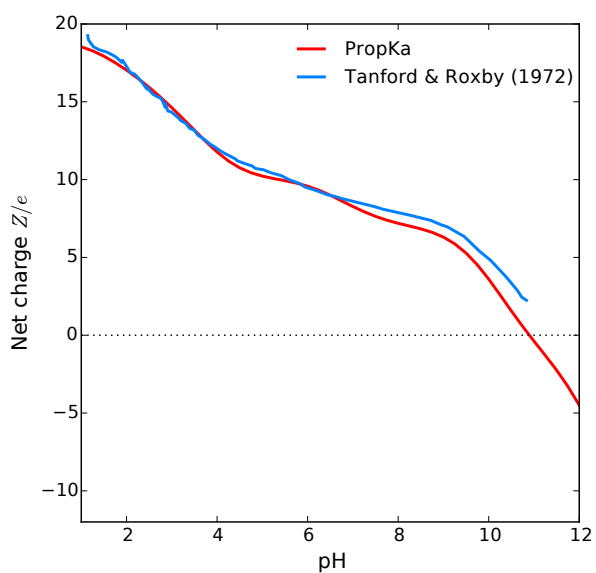


Figure S1: Lysozyme titration curves, obtained with the program PropKa<sup>1,2</sup> using the three-dimensional structure (PDB ID: 2VB1<sup>3</sup>) (red line) or experimentally by Tanford and Roxby in a KCl solution at a 100 mM ionic strength<sup>4</sup> (blue line).

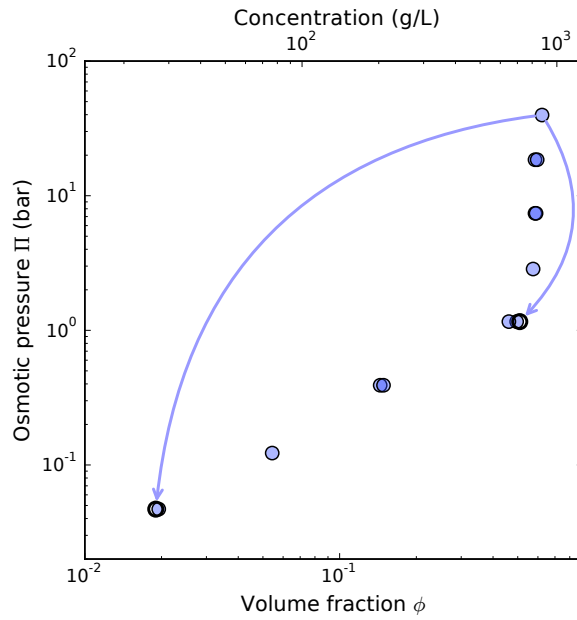


Figure S2: Reversibility of osmotic stress of lysozyme at pH 7,  $I = 150$  mM.  $(\phi, II)$  diagram of lysozyme in a pH 7,  $I = 150$  mM bis-tris propane buffer, obtained by one-way compression (filled blue circles), or by compression to 39.75 bar followed by decompression to 1.16 bar and 0.05 bar (“two-way compression”, empty black circles). The arrows symbolize the decompression part of the two-way compression experiments.

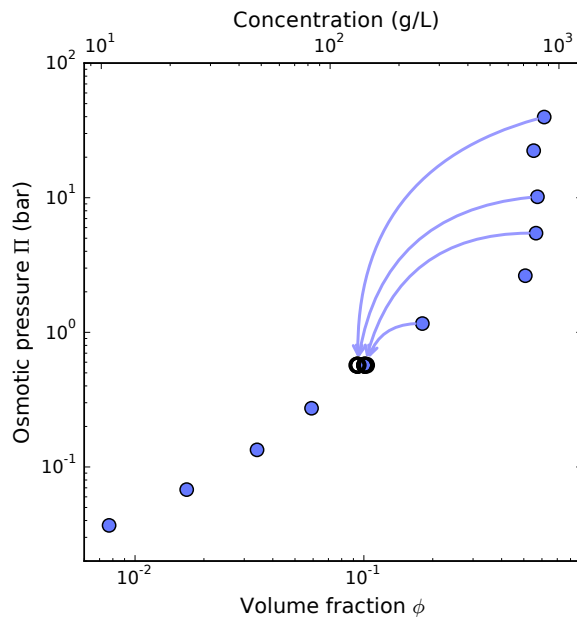


Figure S3: Reversibility of osmotic stress of lysozyme at pH 7,  $I = 35$  mM.  $(\phi, II)$  diagram of lysozyme in a pH 7,  $I = 35$  mM bis-tris propane buffer, obtained by one-way compression (filled blue circles), or by compression to 1.16 bar, 5.45 bar, 10.16 bar and 39.75 bar followed by decompression to 0.57 bar (“two-way compression”, empty black circles). The arrows symbolize the decompression part of the two-way compression experiments.

**Secondary structure of lysozyme (pH 7,  $I = 20$  mM buffer).** Fourier transform infrared spectroscopy (FTIR) is sensitive to the secondary structure of globular proteins. It has been widely used to evidence conformation changes and aggregation of lysozyme<sup>5-12</sup>.

Attenuated total reflectance (ATR) spectra of protein solutions were measured at a  $4\text{ cm}^{-1}$  resolution using a Bruker Tensor 27 spectrometer, a Pike MIRacle ATR accessory equipped with a monoreflexion germanium crystal and a liquid nitrogen-cooled Hg-Cd-Te photovoltaic detector (Bruker). 128 scans were averaged using the Bruker Opus software, and corrected for water vapor and carbon dioxide contributions.

Fig. S4 presents the amide I and amide II region of mid-infrared spectra for lysozyme in pH 7,  $I = 20$  mM buffer. Two of the presented spectra correspond to pressures close to 1.16 bar, reached either through one-way compression, or through two-way compression. Two other spectra correspond to pressures on both sides of the “large volume fraction step”, namely 2.17 bar and two-way compression 7.40 bar. The last spectrum is that of the stock solution of lysozyme at 50 g/L, which serves as a reference sample.

In spite of obvious differences in signal/noise ratio due to large differences in concentration between the reference stock solution and the compressed samples, all the spectra show very similar secondary structures. Indeed, the spectra of the samples belonging to the dilute regime (1.16 bar) and to the concentrated regime (7.40 bar) are almost superimposable, showing that no major change in secondary structure and no aggregation occurs during and after the transition, despite the very high volume fractions attained.

Moreover, we can see that the samples obtained by one-way or two-way compression are identical. Therefore the process of compressing the samples up to the maximum volume fraction (at 39.75 bar) and bringing it back to the initial state does not change the secondary structure of the protein. This structural reversibility corroborates the thermodynamic and morphologic reversibility of the compression discussed above.

**Small-angle X-ray scattering (SAXS).** SAXS experiments were performed on the SWING line of SOLEIL synchrotron, at Gif-sur-Yvette (France). The incident beam wavelength was  $1.0332\text{ \AA}$  (12 keV). We used a detector distance of 1.5885 m for the dilute samples (concentration lower than 10 g/L) and two distances, 5.130 m and 1.130 m, for the concentrated samples. The total  $q$  range spans from  $1.8 \times 10^{-3}\text{ \AA}^{-1}$  to  $0.99\text{ \AA}^{-1}$ .

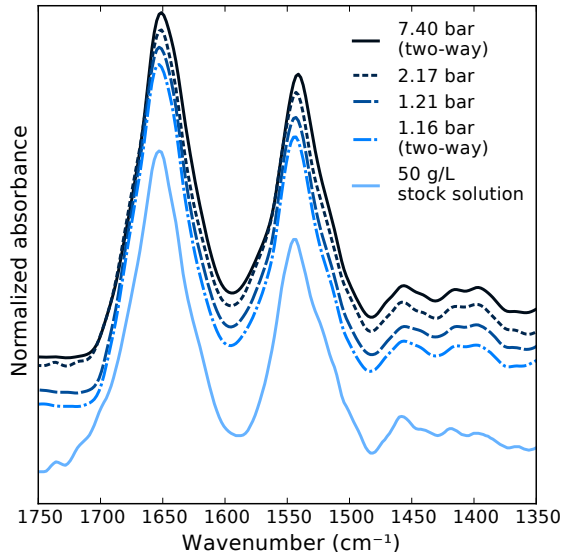


Figure S4: Fourier Transform Infrared Spectroscopy (FTIR) spectra of lysozyme 50 g/L stock solution, and samples compressed to 1.21 bar and 2.17 bar, and decompressed to 1.16 bar and 7.40 bar after compression to 39.75 bar. The spectra were scaled and shifted upwards for better clarity.

The dilute samples were obtained for every physicochemical condition by direct dilution of lysozyme powder in the buffer, in order to attain concentrations of 1 g/L, 2 g/L, 4 g/L, 6 g/L, 8 g/L and 10 g/L. These samples were used to measure the form factor of lysozyme in every physicochemical condition. The concentrated samples were obtained by osmotic compression.

Fitting of the Bragg peak positions was realized with the Fityk software<sup>13</sup> and its module dedicated to powder diffraction analysis, using the Pawley method, i.e. simultaneous optimization of all parameters, the peak positions being constrained by the space group choice. Optimization was performed using the Levenberg-Marquardt algorithm.

**Generalized van der Waals model (GVDW).** Consider a system consisting of  $N$  molecules of radius  $a$  dispersed in a volume  $V$  at constant temperature  $T$ . In a mean field approach the average energy per particle is<sup>14</sup>:

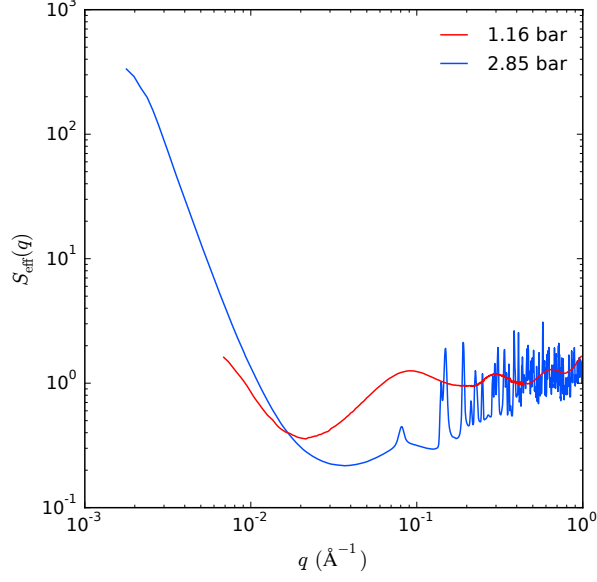


Figure S5: Effective SAXS structure factors of lysozyme solutions compressed to 1.16 bar (red curve) and 2.85 bar (blue curve) in a pH 7,  $I = 20$  mM bis-tris propane buffer.

$$\beta\epsilon = 2\pi\rho \int_0^\infty g(r)\beta w(r)r^2 dr \quad (1)$$

where  $\rho = N/V$  is the bulk number density,  $r$  the interparticle distance,  $g(r)$  the radial distribution function, and  $w$  an effective pair potential.  $\beta = 1/k_B T$  is the reciprocal of the thermal energy. The configurational integral (the static part of the partition function) can now be written as:

$$Z = \int e^{-\beta N\epsilon} d\mathbf{r}^N \quad (2)$$

We now face the problem that the solution structure, described by  $g(r)$ , is unknown and in the GVDW theory a simple step function is assumed: for  $r < 2a$ ,  $g(r) = 0$  while unity otherwise. With this simplification, using Stirling's approximation and neglecting the translational part of the partition function, the system free energy reduces to:

$$\beta A = -\ln \frac{Z}{N!} = N \ln \frac{N}{V - Nv} - N + 2\pi \frac{N^2}{V} \int_{2a}^{\infty} \beta w(r) r^2 dr \quad (3)$$

where  $v = 4\pi a^3/3$  is the particle hard-sphere volume. The final pressure is now obtained as:

$$\beta \Pi = - \left( \frac{\partial \beta A}{\partial V} \right)_T = \frac{N}{V - Nv} + 2\pi \rho^2 \int_{2a}^{\infty} \beta w(r) r^2 dr \quad (4)$$

The above offers a molecular interpretation of the original van der Waals equation of state, where in the first term of purely entropic origin,  $b = v$ . The second term accounts for the mean interaction energy per particle,  $K = -2\pi \int_{2a}^{\infty} \beta w(r) r^2 dr$ . Here it should be noted that  $K$  may include both attractive and repulsive interactions and can be evaluated for any pair potential that decays as  $1/r^3$  or faster.

The first term can be replaced by the Carnahan-Starling expression,  $\rho \frac{1+\phi+\phi^2-\phi^3}{(1-\phi)^3}$ , and the bulk number density be expressed as  $\rho = \phi/v$ .

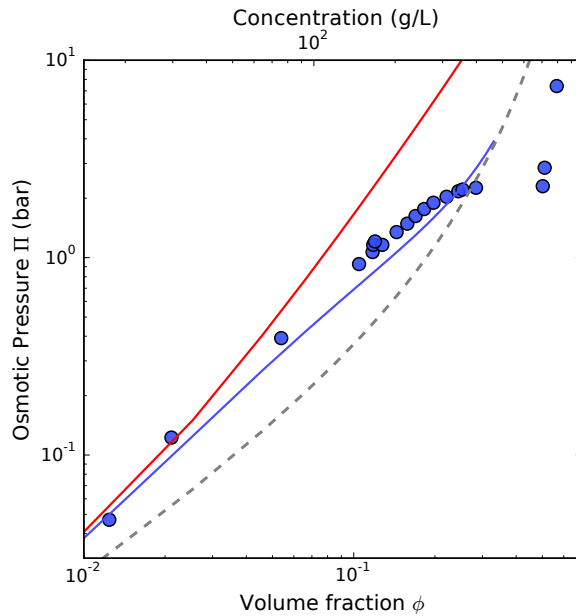


Figure S6: Generalized van der Waals (GVDW) model : contribution of lysozyme counterions to the screening of electrostatic interactions. The GVDW model, with (blue line) or without (red line) the contribution of lysozyme counterions to the effective ionic strength, was fitted globally to the dilute regime of experimental osmotic pressure *vs.* volume fraction data of lysozyme at pH 7,  $I = 20$  mM; pH 7,  $I = 35$  mM; pH 7,  $I = 150$  mM and pH 9,  $I = 20$  mM. For clarity, the experimental data and fitted models are plotted only for pH 7,  $I = 20$  mM. The value of the adjusted Hamaker constant is  $3.76 k_B T$  and  $10.82 k_B T$  with and without contribution of counterions, respectively (for numerical integration of the interaction term, the lower limit was increased by 0.02 nm to avoid divergence). The model lines are plotted only in the volume fraction range used for the fit. The grey dashed line represents the Carnahan-Starling model.

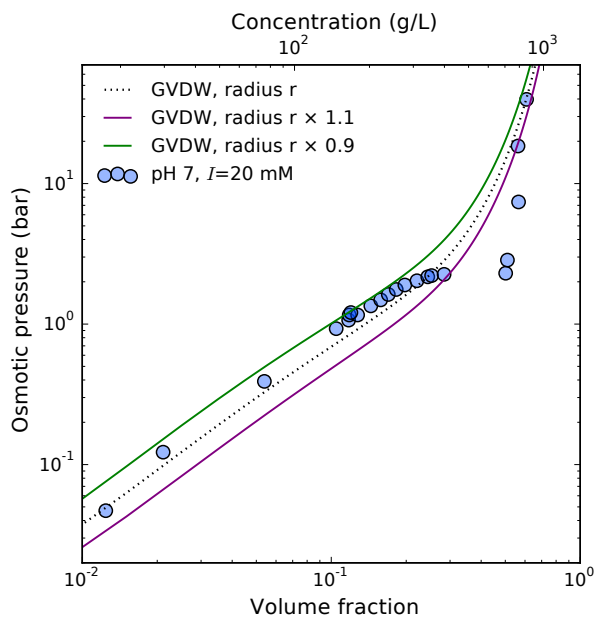


Figure S7: Impact of the value of the radius of the lysozyme model on the osmotic pressure predicted by the generalized van der Waals (GVDW) model. Together with the experimental osmotic pressures obtained at pH 7,  $I=20$  mM (circles) and the fit of the GVDW model as in the manuscript, fig. 4 (dotted line), the GVDW model is also plotted for a model sphere with a radius 10% higher (purple line) or lower (green line) than the radius calculated from lysozyme mass and specific volume.

## References

- [1] H. Li, A. D. Robertson and J. H. Jensen, *Proteins: Struct., Funct., Bioinf.*, 2005, **61**, 704–721.
- [2] M. H. M. Olsson, C. R. Søndergaard, M. Rostkowski and J. H. Jensen, *J. Chem. Theory Comput.*, 2011, **7**, 525–537.
- [3] J. Wang, M. Dauter, R. Alkire, A. Joachimiak and Z. Dauter, *Acta Crystallogr., Sect. D*, 2007, **63**, 1254–1268.
- [4] C. Tanford and R. Roxby, *Biochemistry*, 1972, **11**, 2192–2198.
- [5] R. J. Green, I. Hopkinson and R. A. L. Jones, *Langmuir*, 1999, **15**, 5102–5110.
- [6] S. D. Allison, B. Chang, T. W. Randolph and J. F. Carpenter, *Arch. Biochem. Biophys.*, 1999, **365**, 289–298.
- [7] A. Dong, T. W. Randolph and J. F. Carpenter, *J. Biol. Chem.*, 2000, **275**, 27689–27693.
- [8] F. Meersman and K. Heremans, *Biochemistry*, 2003, **42**, 14234–14241.
- [9] A. Hirano, H. Hamada, T. Okubo, T. Noguchi, H. Higashibata and K. Shiraki, *Protein J.*, 2007, **26**, 423–433.
- [10] A. Sethuraman and G. Belfort, *Biophys. J.*, 2005, **88**, 1322–1333.
- [11] P. Sassi, A. Giugliarelli, M. Paolantoni, A. Morresi and G. Onori, *Biophys. Chem.*, 2011, **158**, 46–53.
- [12] Y. Zou, Y. Li, W. Hao, X. Hu and G. Ma, *J. Phys. Chem. B*, 2013, **117**, 4003–4013.
- [13] M. Wojdyr, *J. Appl. Crystallogr.*, 2010, **43**, 1126–1128.
- [14] S. Nordholm, *Properties of Molecular Fluids in Equilibrium*, Lecture notes, 2014.